REPORT NO. 30-8

WELDED TITANIUM CASE FOR SPACE-PROBE ROCKET MOTOR

A. J. BROTHERS
R. A. BOUNDY
H. E. MARTENS
L. D. JAFFE

JET PROPULSION LABORATORY
CALIFORNIA INSTITUTE OF TECHNOLOGY
PASADENA, CALIFORNIA
SEPTEMBER 3, 1959

REPORT NO. 30-8

WELDED TITANIUM CASE FOR SPACE-PROBE ROCKET MOTOR

A. J. Brothers
R. A. Boundy
H. E. Martens
L. D. Jaffe

Leonard D. Jaffe
Leonard D. Jaffe, Chief
Materials Research Section

Copy No.__________
This document contains
cover and 6 leaves.

JET PROPULSION LABORATORY
California Institute of Technology
Pasadena, California
September 3, 1959

CONTENTS

TABLES

FIGURES

PREFACE

Portions of the following report were originated under studies conducted for the Department of Army Ordnance Corps under Contract No. DA-04-495-Ord 18. Such studies are now conducted for the National Aeronautics and Space Administration under Contract No. NASw-6.

ABSTRACT

The high strength-to-weight ratio of titanium alloys suggests their use for solid-propellant rocket-motor cases for high-performance orbiting or space-probe vehicles. The paper describes the fabrication of a 6-in.-diam., 0.025-in.-wall rocket-motor from the 6Al–4V titanium alloy. The rocket-motor case, used in the fourth stage of a successful JPL-NASA lunar-probe flight, was constructed using a design previously proven satisfactory for Type 410 stainless steel. The nature and scope of the problems peculiar to the use of the titanium alloy, which effected an average weight saving of 34%, are described.

I. INTRODUCTION

Early in 1958, the Jet Propulsion Laboratory of the California Institute of Technology was requested to participate in a lunar-probe mission code-named *Juno II,* which would place a 15-lb instrumented payload (*Pioneer IV*) in the vicinity of the moon. The vehicle was to use the same high-speed-upper-stage assembly as flown on the successful *Jupiter-C* configuration; however, the first-stage booster was to be a *Jupiter* rather than a *Redstone*. An analysis of the intended flight and payload configuration indicated that the feasibility of accomplishing the mission was questionable and that additional performance would have to be obtained if the mission was to be feasible.

Since the most efficient way of increasing the performance of a staged vehicle is to increase the performance of the last stage, a study of possible ways of doing this was made. Because of the time schedule placed on this effort it was decided to reduce the weight of the fourth-stage rocket-motor case by substituting the annealed 6Al–4V titanium alloy[1] for the Type 410 stainless steel.[2] Although this introduced an unfamiliar material, it reduced the changes in design and fabrication techniques. This particular titanium alloy was chosen on the basis of previous tests which proved the suitability of the alloy as a pressure-vessel material when used at an annealed yield strength of about 120,000 psi.

[1] 6Al–4V titanium alloy has a nominal composition of 6% aluminum, 4% vanadium; balance is titanium.

[2] Type 410 is a martensitic stainless steel with a nominal composition of 12.5% chromium, 0.15% carbon; the balance is iron.

II. DETAILS OF THE MOTOR CASE

The titanium-cased fourth stage of *Juno II* is shown with the payload and on the missile in Fig. 1; the stainless-steel motor cases used in the *Jupiter-C* vehicle are shown in Fig. 2. The fourth-stage motor case has a diameter of 6-in., a length of approximately 38-in., and a nominal cylindrical wall thickness of 0.025-in. As shown in Fig. 1, the case serves as the structural support of the payload and is aligned to the upper stage assembly through an alignment ring. The nozzle is threaded into the end of the motor case, and is of the ceramic-coated steel design.

Figure 3 shows a comparison of the components used to make the stainless steel and the 6Al–4V titanium alloy cases. The forward dome and aft fitting for the stainless steel assembly were fabricated from a combination of forged, spun and machined parts. In order to facilitate the fabrication of the titanium alloy motor, these components were machined from a large-diameter billet.

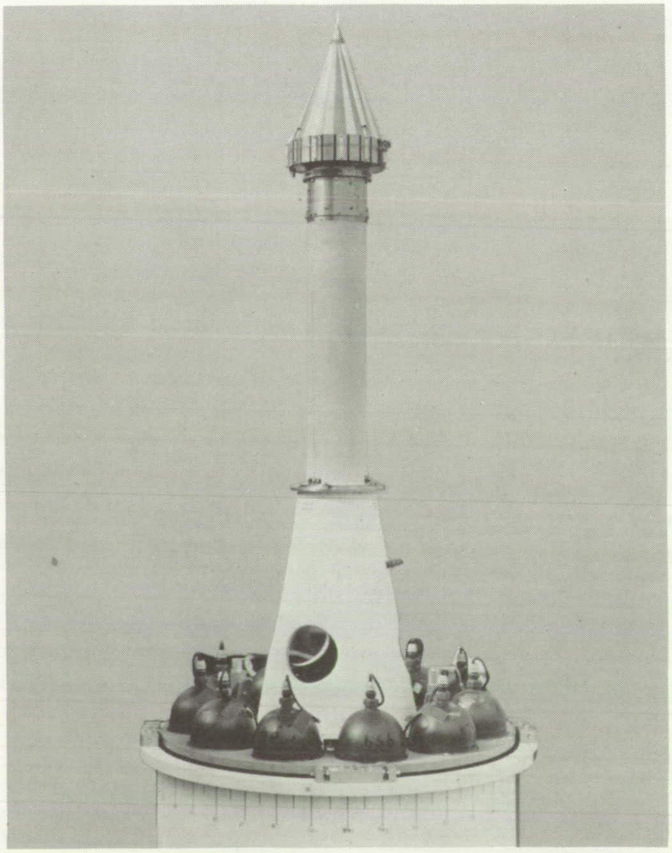

Fig. 1. Moon-Probe Vehicle Showing *Pioneer IV* Mounted on Titanium-Cased Fourth-Stage Rocket Motor

Fig. 2. Stainless-Steel *Jupiter-C* Upper Stage Motor Cases

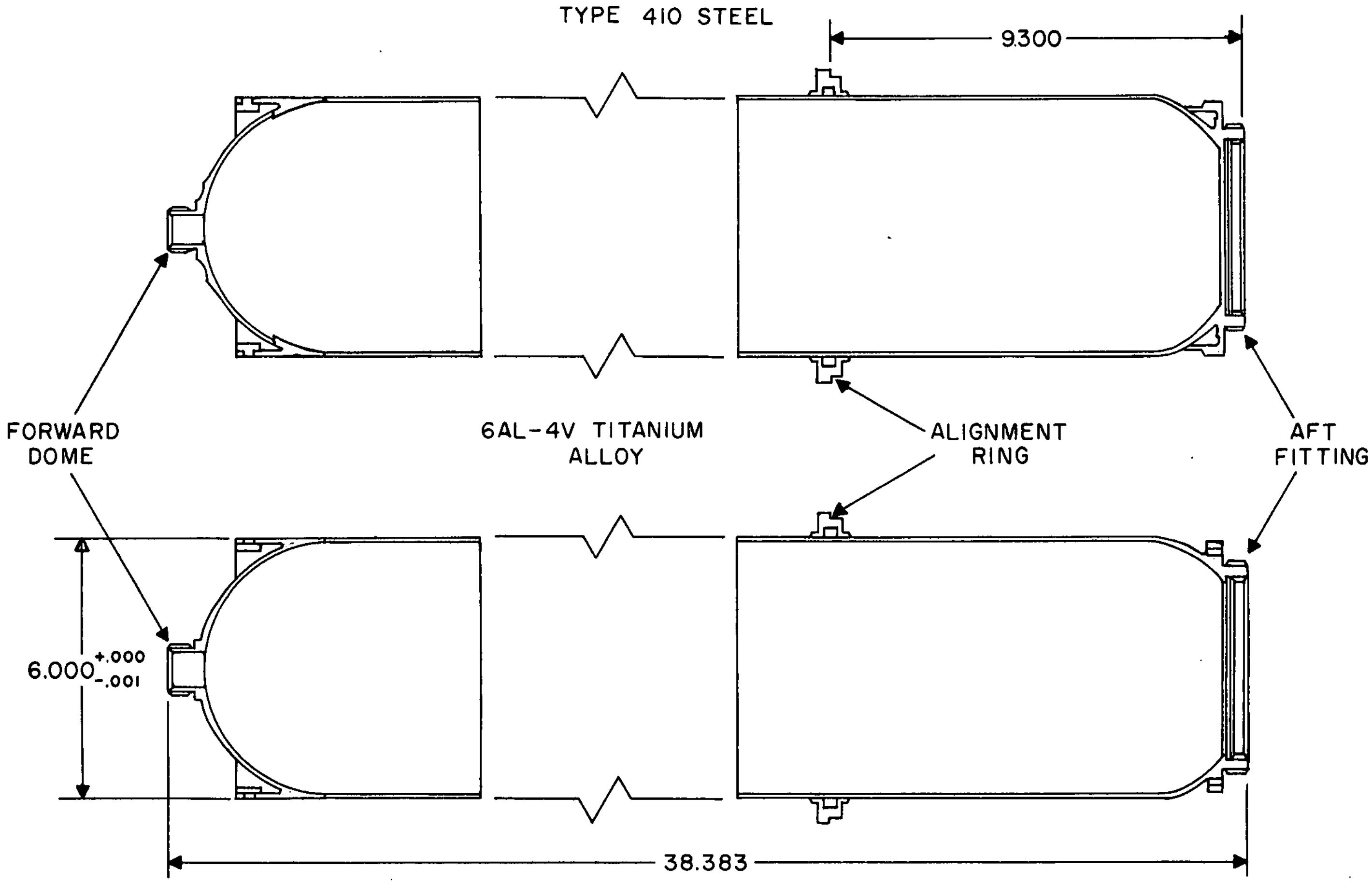

FORWARD DOME AND AFT FITTING OF TYPE 410 STEEL CASE CONSTRUCTED OF THREE PIECES WELDED TOGETHER. CORRESPONDING COMPONENTS OF 6AL-4V TITANIUM ALLOY CASE WERE MACHINED FROM 6.5 INCH DIAMETER BILLET.

Fig. 3. Comparison of 6Al–4V Titanium-Alloy and Type 410 Stainless-Steel Fourth-Stage Motor Cases

III. FABRICATION OF THE TITANIUM-ALLOY MOTOR CASE

A completed fourth-stage rocket motor case fabricated from the titanium alloy is shown in Fig. 4. The details of the various fabrication operations are depicted in Figs. 5 through 11. Table 1 describes the welding procedures used.

Figure 5 shows a sizing jig being used to finish the 6-in.-diam. rolled shell. Because of its high annealed yield strength and considerable "spring-back" the titanium alloy could not be hand formed at room temperature as was the stainless steel, but required use of the jig. By maintaining good joint fit, a high degree of cleanliness, and adequate gas shielding, the longitudinal weld could be done without an enclosure, as shown in Fig. 6.

During the initial phases of the fabrication program it was determined that if extreme care was used, all circumferential welds could be made in an open-topped trough which was purged with argon prior to and during welding. However, as the fabrication became more extensive it was decided that a system requiring less care and time would have to be developed. Such a system is shown in Fig. 7. It utilizes a long plastic bag reinforced at the seams with glass-fabric tape and supported at the weld site with a sheet-metal bridge. This system was simple to construct, easily purged and capable of providing a satisfactory atmosphere. The 5-by-7-in. opening in the bridge allowed the welder convenient access to the three joints to be welded in each motor case. A suitable protective shield was obtained by means of a slightly positive gas flow.

Fig. 4. Completed Weldment of Titanium-Alloy Motor Case

Figures 8 and 9 illustrate tacking and welding of the alignment ring. This weld required no filler metal, since a flange was provided on each edge of the ring for fusing to the shell. Although the final welding was carried out

Table 1. Preparation and Technique for Welding Titanium-Alloy Rocket-Motor Case

Step or Item	Longitudinal Weld	Support-Ring Weld	Forward and Aft Dome Welds
Filler Wire	0.030-inch diam. 6Al–4V titanium-alloy wire	None	0.030-in. diam. 6Al–4V titanium-alloy wire
Welding Procedure	Manual	Semi-automatic	Semi-automatic
Cleaning Procedure	Buff with felt wheel, acetone degrease, rinse with hot water		
Joint Backing	Grooved copper (0.030-in.-deep-by-¼-in. wide groove)	expanding copper back-up, no groove	expanding copper back-up, no groove
Inert-Gas Shielding Used, cfh			
Torch (Argon)	12	12	12
Back-up (Argon)	2.5	2.5	2.5
Welding Speed, ipm	4	5	4
Torch and cup	Commercial, water-cooled copper cup, 2 in. long by 0.75 in. ID on commercial air-cooled hand welding torch		
Electrode	Pointed 0.040-in. diam thoriated tungsten with 0.30-in. extension from torch cup		
Amperage	70	70	70

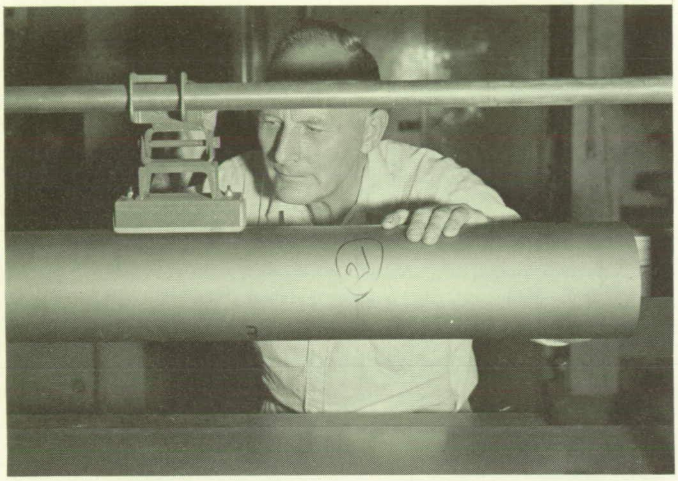

Fig. 5. Final Sizing of Titanium-Alloy Shell

Fig. 6. Seam-Welding Titanium-Alloy Shell

in the plastic chamber, the tacking was performed without an enclosure. Improper fit-up between the ring and the shell resulted in low cooling rates and shrinkage distortion, both of which caused weld contamination. To keep this contamination at a minimum, short segments of the ring were welded 180 deg apart and along opposite edges until the entire weld was complete.

A circumferential weld typical of the forward and aft dome welds is illustrated in Fig. 10. This figure shows the forward dome being tack-welded to the shell subassembly. This weld was actually performed in the plastic chamber but for the purpose of clarity is shown being performed in air. An expanding copper back-up mandrel and copper chill rings were used to control the cooling rate of the weld. The cooling rate was very important; if it was too rapid, there was a greater incidence of porosity; if it was too slow, the weld metal discolored, indicating possible contamination.

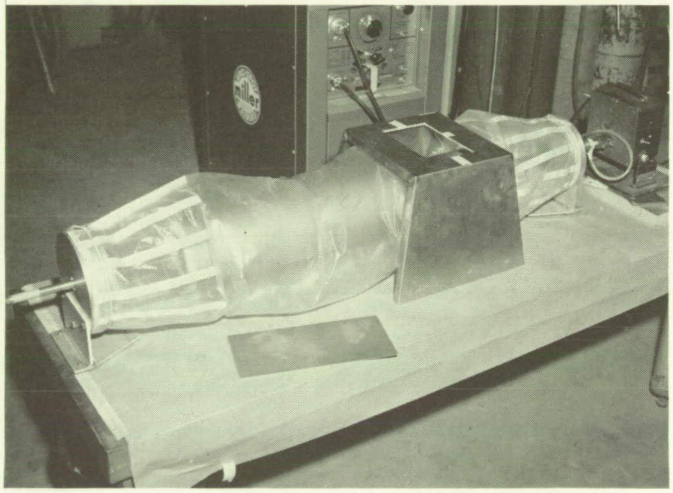

Fig. 7. Plastic Enclosure Used to Weld Titanium Motor Case

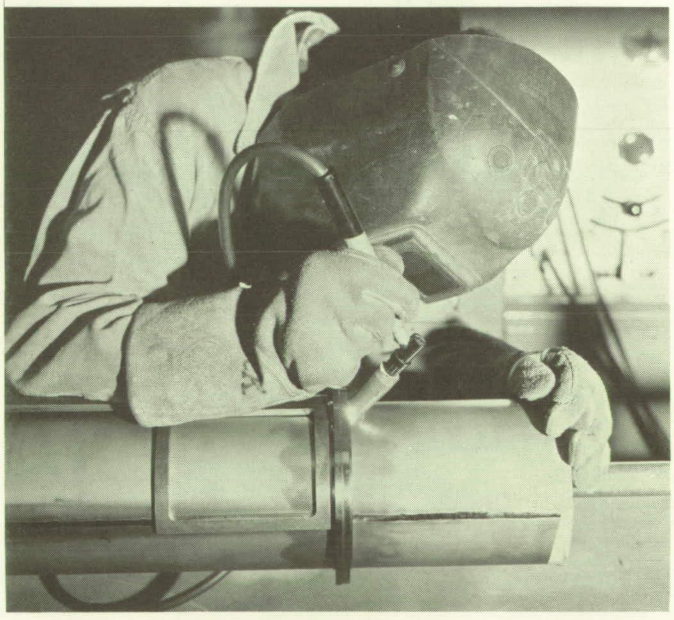

Fig. 8. Tack-Welding Alignment Ring to Shell

Fig. 9. Welding Alignment Ring to Shell

Fig. 10. Tack-Welding Forward Dome to Shell

As shown in Fig. 1, the *Pioneer IV* payload was attached to the forward skirt of the fourth-stage motor. To conserve weight, nut plates were used to make this attachment. These nut plates were bonded to the titanium alloy with an epoxy adhesive, since soldering is not a simple procedure on titanium alloys.

Protection of the forward and aft domes from overheating due to exposure to hot combustion gases was accomplished by spraying the interior surfaces of these domes with a commercial zirconia coating approximately 0.020-in. thick.

After case fabrication, nut-plate attachment, and ceramic coating, the rocket motor cases were lined and cast with solid propellant, and firing diaphragms were placed between nozzle and case. Since the igniter used had greater reliability when used at atmospheric pressure, it was desirable to seal the completed motor case until ignition. The use of a coined copper diaphragm designed to provide this seal at the nozzle end of the Type 410 stainless-steel case was questionable on the titanium case because of the known low-melting copper-titanium eutectic. Rather than change the diaphragm material, the copper was nickel plated on the surface which contacted the titanium-case seat.

IV. EVALUATION TESTS

In order to prove the design and fabrication of the 6Al–4V titanium alloy as a material of construction, each completed motor case was hydrostatically proof-tested. This test consisted of three cycles up to 830 psi with a 5-minute hold at pressure for each cycle. This pressure corresponds to a calculated hoop stress of about 100,000 psi. Of 26 cases fabricated and proof tested, only one case failed to pass the hydrostatic test. In this one case, failure occurred at 830 psi on the first cycle and was evident as a small crack approximately 0.5 inches long in the longitudinal seam weld and parallel to it near the intersection with the support-ring weld. The crack was associated with a previously undetected area of weld contamination at the intersection of the longitudinal and support ring welds.

Of the 26 cases fabricated and proof-tested, 16 were statically fired, all successfully. These tests expose the motor case to conditions of rapid loading and high-temperature, high-velocity gases and provide an indication of the reliability of the case material. In addition to ambient temperature firings, a case each was fired at 30° and 120° F to prove firing capability under these conditions. In order to prove the capability of reusing once-fired cases, two cases were reloaded and refired with satisfactory performance.

In addition to hydrostatic and static-firing proof tests, five cases were hydrostatically tested to rupture. These test results are shown in Fig. 11 and Table 2. The curves of Fig. 11 show the increase in volume as a function of pressure for three of five motor cases tested to rupture. These measurements were obtained by pressurizing the tanks with water taken from a calibrated standpipe. The deviation from linearity of the volume-pressure curve is interpreted as bulk yielding and represents high ductility of the motor case in the presence of biaxial loading. The variation in pressure at which fracture occurred resulted from different sheet thickness and strength properties which are shown in Table 2. This table compares all of the cases which have been hydrostatically tested to rupture and shows the nominal calculated hoop stress based on the fracture pressure, the ultimate strength of material from locations near the area from which the case material was taken, and the ratio of these two values. Since the hoop-stress calculation is based on an elastic stress relationship, it is not directly applicable in the plastic regime.

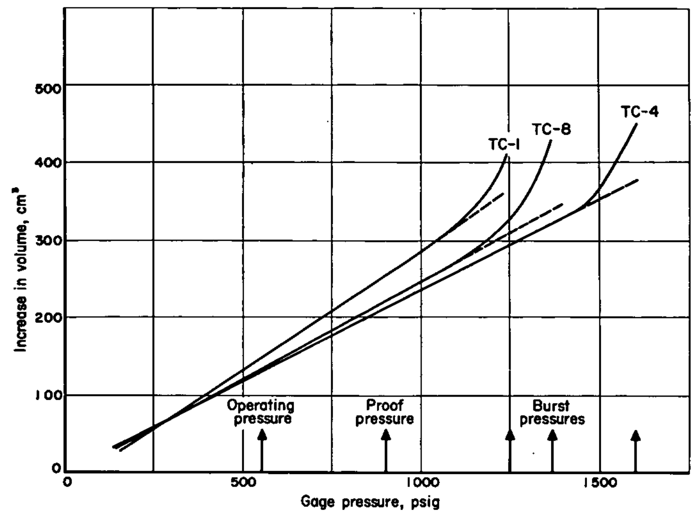

Fig. 11. Increase in Volume during Hydrostatic-Pressure Test of Titanium-Alloy Motor Case

Table 2. Hydrostatic-Pressure Test Results of 6Al-4V Titanium-Alloy Motor Cases

Test No.	Condition	Burst Pressure psi	Calculated Hoop Stress At Rupture ksi	Ultimate Tensile Strength ksi	Average Sheet Thickness in.	Ratio of Calculated Stress to Tensile Strength
TC-1	As fabricated	1250	151.5	126.5	0.025	1.20
TC-4	As fabricated, then stress-relieved[a], then statically fired	1600	166.5	141.9	0.029	1.17
TC-3	Statically fired	1630	174.5	136.4	0.028	1.28
TC-8	Statically fired	1370	166.5	137.8	0.025	1.21
TC-10	Statically fired	935	111.0	136.6	0.025	0.81

[a]Stress-relieved at 1150° F, 1.5 hr, air-cooled.

It does, however, provide a means of comparing the results of cases of unequal thickness or material-strength level.

Except for TC-10, which failed at a low pressure at an obvious stress concentration resulting from excessive repair welding, the ratio of calculated hoop stress to ultimate strength is approximately 1.2. It is of interest to note that TC-4, which was stress-relieved at 1150° F for 1.5 hours, was similar in behavior to those cases which had not been stress-relieved subsequent to fabrication.

V. WELDING DEFECTS

Although there were a number of common defects such as burn-throughs, tungsten inclusions, incomplete penetration, etc., the defect of greatest concern was weld porosity. The need for extremely careful cleaning procedures became apparent in preliminary tests of longitudinal seam welds during which it was noted that joints cleaned with the procedures listed in Table 1 invariably contained much less porosity than those merely degreased prior to welding. It was not possible, however, to completely eliminate porosity by scrupulous cleaning techniques.

It is of interest to note that the greatest incidence of porosity occurred in the support-ring weld. This weld was exceptional in that fit-up between the ring and shell was quite often poor. In another instance, porosity was found in the weld of a loose-fitting forward dome and suggests that fit-up as well as cleaning may have an effect on weld porosity. It was also observed that porosity was often associated with narrow areas of the weld. This suggests that a high cooling rate in these areas may not have permitted a porosity-forming medium to leave the molten weld metal. For this reason, where possible, welds were made with high heat input.

There is some evidence in the literature that weld porosity can be removed by remelting the weld area in which it occurs. Preliminary tests indicated that this was the case and that remelting was not detrimental to the hydrostatic test properties of a cylindrical pressure vessel of this alloy. Remelting was attempted on two cases containing porous welds. One remelting operation resulted in compounding the defect. In the second instance, porosity was reduced but not eliminated.

Five motor cases with known areas of weld porosity were hydrostatically tested to rupture. In no case could fracture be associated with this defect. Several other cases which contained weld porosity rejectable by radiographic inspection were proof-tested and statically fired sucessfully.

VI. CONCLUSION

The weight saving realized by substitution of the 6Al–4V titanium alloy was 2.8 lb, or a weight-reduction of approximately 34% over the heat-treated Type 410 stainless-steel motor case. This increased performance, which could have been translated into either greater payload weight or an increase in the potential maximum velocity of the payload, was used to extend the permissible launching time, thereby increasing the probability of a successful flight. Without the increased fourth-stage capability provided by the use of the lighter-weight titanium-alloy motor case, this flight mission would not have been attempted.